Ceramic Transactions, v.83, pp.375-382 (1998)

ASSESSMENT OF THE CRITICAL THICKNESS AND FRACTURE TOUGHNESS OF THIN METAL-ORGANIC PRECURSOR FILMS

Ryan K. Roeder and Elliott B. Slamovich
School of Materials Engineering, Purdue University, West Lafayette, IN 47907-1289

ABSTRACT

A fracture mechanics approach for the study of cracking in thin films was demonstrated. The drying and cracking of thin metal-organic precursor films were examined by monitoring film thickness and evaporative mass loss. Experiments and calculations revealed two methods to prevent film cracking: (1) choosing a precursor to minimize evaporative stress during drying, and (2) adding elastomeric polymers to the precursor to increase the film fracture toughness.

INTRODUCTION

Sol-gel, metallo-organic decomposition, and hydrothermal routes to ceramic thin films depend on the mechanical integrity of the precursor film. The mechanical integrity of thin films has long been observed to be dependent on the film thickness. The critical film thickness for cracking is system and material dependent, reflecting the film fracture toughness. The critical film thickness has typically been observed in the range of 0.4 - 1.0 μm for a variety of materials and conditions.[1-6] Films above the critical thickness are observed to crack or decohere from the substrate. Cracking is caused by internal stresses that exceed the film's cohesive strength, and decoherence is due to stresses that exceed the adhesive strength to the substrate.[6-9]

Internal stresses in thin films arise from a material's response to constrained volume changes.[8,9] Constrained volume changes occur during many processes including drying, thermal expansion or contraction, pyrolysis, densification and curing. The internal strain induced by a constrained volume change is calculated as

$$\varepsilon = \frac{\Delta l}{l} = \left(1 + \frac{\Delta V}{V}\right)^{1/3} - 1. \qquad (1)$$

Assuming primarily elastic behavior (e.g. a small plastic zone), the internal biaxial film stress is given as

$$\sigma = \frac{E \cdot \varepsilon}{1 - \nu} = \frac{E}{1 - \nu} \cdot \left[\left(1 + \frac{\Delta V}{V}\right)^{1/3} - 1\right], \qquad (2)$$

where E is the film's elastic modulus and ν is Poisson's ratio.

Brittle films under a tensile stress are observed to crack or decohere from the substrate when above the critical thickness. The Griffith criterion for cracking in

brittle solids shows that the stress required for fracture is inversely related to the film thickness, based on a macroscopic energy balance between the stress relieved and surfaces created during crack propagation. Thus, the Griffith criterion accounts for the critical thickness phenomenon, but is not alone sufficient. The stress concentration at the crack tip must also be considered because the cohesive strength of a material must be overcome on the atomic scale. The stress concentration required for crack propagation is described by the critical stress intensity factor (K_c), which is a geometry dependent material property. Evans and co-workers[10,11] used linear elastic fracture mechanics to predict the critical film thickness, h_c, in terms of K_c for a thin film as

$$h_c = \left(\frac{K_c}{\sigma \cdot \Omega}\right)^2, \text{ where } \Omega \propto \sqrt{\pi \cdot \left(\frac{E}{E_s}\right)}. \qquad (3)$$

σ is the film stress and Ω is a semi-empirical non-dimensional parameter related to the ratio of elastic moduli for the film (E) and substrate (E_s). Eq. (3) predicts film cracking when the film thickness is greater than or equal to h_c. In this study, K_c for a thin film under mode I loading is expressed as "K_{Ic}" to denote *plane stress* and to differentiate from the commonly misused notation for *plain strain*, "K_{Ic}."

The above concepts of thin film fracture mechanics were used in the following experimental study of cracking in thin metal-organic precursor films. Rather than using Eq. (3) to predict the critical thickness for cracking, the critical thickness was measured and Eq. (3) used to examine the origins of film cracking. The drying and cracking of precursor films were examined by monitoring film thickness and evaporative mass loss. Internal film strains were calculated from the constrained volume shrinkages. Estimates of the normalized film stress and relative fracture toughness were used to identify processing effects on the cracking behavior. Cracking was prevented (increased critical thickness) by either minimizing the evaporative stress during drying, or toughening the precursor film via elastomeric polymer additions.

EXPERIMENTAL PROCEDURE

Two metal-organic precursors were investigated: titanium di(isopropoxide) bis(ethyl acetoacetate) (TIBE) and titanium dimethoxy dineodecanoate (TDD). Both have been used to process titanate thin films for microelectronic applications.[13-16] TIBE is known to crack readily,[13] while TDD does not. For spin coating, TIBE and TDD were diluted in 50 vol% toluene and 70 vol% p-xylene, respectively, such that the solution viscosities were nearly equal for shear rates of 1 to 1000 s^{-1}. TIBE solutions were further modified by dissolving 5.0 and 10.0 wt% (relative to TIBE) of an elastomeric styrene-butadiene-styrene block copolymer (Kraton® D1102C, Shell Oil Co.). The viscosity before and average film thickness after spin coating increased with polymer content. Also, two control solutions were prepared: as-received TIBE without solvent dilution and TIBE diluted in 50 vol% p-xylene. All films were spin coated in a forced convection fume hood at 5000 rpm for 15 s on Pt-coated glass substrates. The Pt coating provided reflectance for obtaining optical interference fringes and infrared spectra. Additional details of the TIBE solutions, spin coating procedure and viscosity measurements are available in Ref. 12.

Drying took place at room temperature and atmospheric pressure. The substrate mass was recorded beforehand so the film mass could be measured during drying. The film mass was monitored during drying using a microbalance (±0.005 mg), taking measurements 0.1, 0.5, 1.0, 1.5, 2.0, 2.5, 3.0, 4.0, 12.0, and 90 h after spin coating. The film morphology, including film thickness, crack initiation, crack growth, and crack arrest, was simultaneously observed using a standard optical microscope. Isochromatic color fringes resulting from optical interference of light reflected from the film and substrate were used to determine film thickness (Fig. 1). The critical thickness measurement technique is discussed in detail in Ref. 12.

Organic compounds present before and after spin coating were identified from infrared spectra obtained using a Fourier transform infrared (FTIR) spectrometer (Magna IR Spectrometer 55, Nicolet Analytical Instruments). The spectra of solvents, precursors, and precursor solutions alone were measured in transmittance by pressing a thin liquid film between NaCl plates. The spectra of films were measured in reflectance at time intervals beginning immediately after spin coating.

Films were subjected to a scratch test to determine the drying time when precursor films underwent a transition from behaving *primarily* as a viscous liquid to an elastic solid. After spin coating, films were lightly scratched with a pair of precision forceps at 5 min time intervals. The response of precursor films was observed in an optical microscope and micrographs were taken after 1 h of drying.

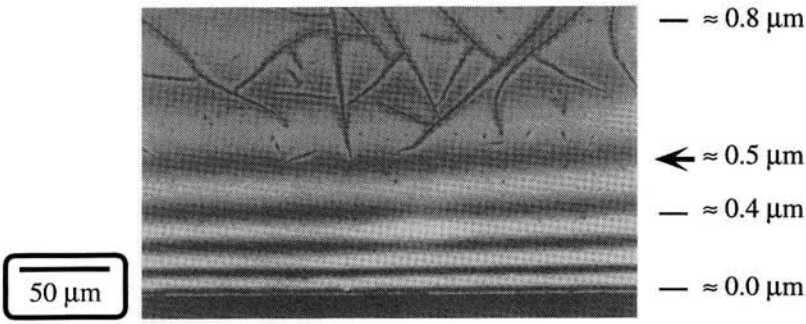

Fig. 1. Optical micrograph of a film made from the TIBE-50 vol% toluene solution with 5.0 wt% (relative to TIBE) polymer after drying 90 h. Cracks terminate at isochromatic color fringes corresponding to the critical film thickness. Note the substrate edge is located along the bottom side of the micrograph.

RESULTS AND DISCUSSION

Microstructural Observations

Observations of the cracking behavior and measurement of the critical thickness of TIBE films have been documented.[12] Crack growth in each film was observed to be complete after 90 h of drying. After 90 h drying, all TIBE films without polymer additions had largely decohered from the substrate; however, crack arrest was observed in the thinnest regions of the film (e.g. the outer edges of the substrate). TIBE films with polymer additions did not decohere. More importantly, cracking was much less widespread with increased polymer content,

despite increased average film thickness as shown by color fringes. Unlike TIBE films, the TDD film did not crack, despite having the largest film thickness.

The critical thickness for films of each precursor solution was determined from micrographs taken where cracks initiating in thicker regions grew into thinner regions (e.g. Fig. 1). The critical thickness was measured as the thickness at which propagating cracks terminated. Ref. 12 discusses optical interference and explains the measurement of the critical film thickness from isochromatic color fringes. The critical thickness measured for each film is listed in Table I. The critical film thickness for cracking increased with increasing polymer content. Note the values reported in Table I contain up to 10% error inherent in the measurement technique. The critical thickness of TDD films could not be determined because these precursor films did not crack, even for films 50 μm thick.

Solvent/Precursor Evaporation

The measured mass of films during drying is shown in Fig. 2. All TIBE films exhibited similar behavior, while the TDD film lost relatively little mass. Decreases in the mass of the TIBE alone indicated that TIBE itself was volatile. An empirical exponential decay equation was used to fit the mass loss data, with film mass (M) as a function of drying time (t), $M(t) = A + B \cdot exp(-C \cdot t)$, as shown in Fig. 2.

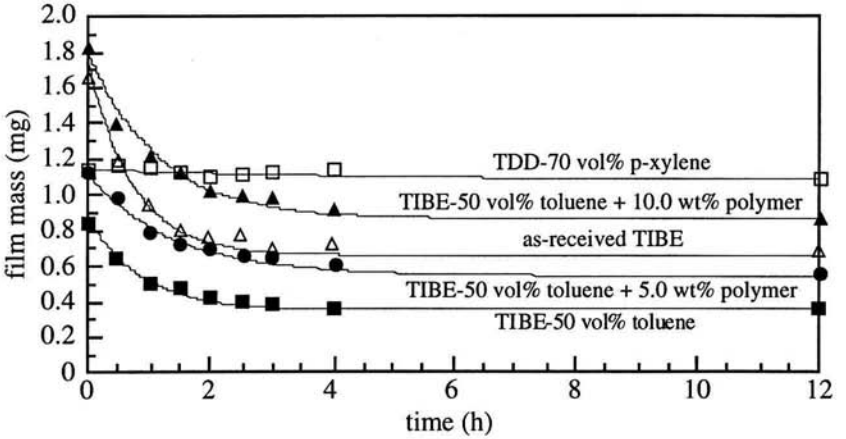

Fig. 2. Film mass for each precursor solution versus drying time, showing mass loss due to evaporation of volatile organics.

The evaporative mass losses were further investigated using FTIR. The FTIR spectra measured for films immediately after spin coating and after short drying times showed no presence of the identified solvent peaks. Thus, virtually all the solvent for each precursor solution evaporated during spin coating. Complete evaporation of solvents during spin coating was facilitated by the relatively high vapor pressures of toluene and p-xylene at room temperature, and the highly convective conditions while spinning at 5000 rpm in a forced convection fume hood. Thus, the origin of the mass loss in TIBE films remained uncertain, possibly

due to the evaporation of TIBE itself, unreacted ethyl acetoacetone (5% in as-received TIBE[17]), or condensation products. In contrast, the negligible mass loss in the TDD film during drying indicated that TDD and its condensation products (if any) had a lower vapor pressure under the drying conditions.

Film Strain, Stress and Fracture Toughness

The scratch test was a simple and effective means to determine the glass transition* of a viscous liquid film to an elastic solid film. Shortly after spin coating scratches completely healed (Fig. 3, 13 min), as the precursor film retained a low viscosity. The response of the film became increasingly viscous for successive scratches, shown by film uplift alongside scratches (Fig. 3, 18 to 28 min). The transition into primarily elastic behavior was determined when no surface uplift was observed and scratch edges were serrated (Fig. 3, ≥ 28 min), indicative of elastic mixed-mode fracture. The approximate drying times to the glass transition (t_g) of precursor films are listed in Table I.

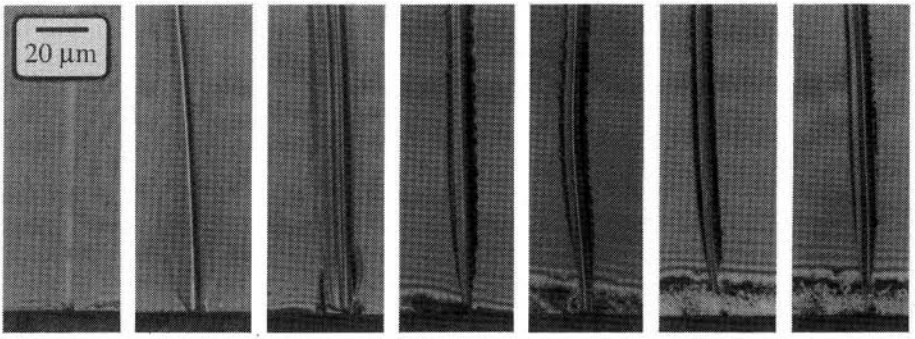

Fig. 3. Optical micrographs (taken after drying 1 h) of a film made from the TIBE-50 vol% toluene solution after performing the scratch test, showing the change in mechanical response from primarily viscous to primarily elastic with increased drying time. The substrate edge is located at the bottom of micrographs.

The measured mass loss and time to glass transition during drying were used to determine the internal strain and stress in each film. Film volume as a function of drying time, $V(t)$, was calculated from the mass loss data using the known densities and initial amounts of constituents in each precursor solution. Internal film strains were determined using Eq. (1) for the volume change that occurred after the glass transition at t_g. The volume change was determined from the film volume at the time of glass transition, $V(t_g)$, and after reaching a steady state, V_∞ (taken at 90 h). The internal linear strains are shown in Fig. 4a and Table I. The corresponding film stresses (Fig. 4a and Table I) were estimated using Eq. (2), normalizing to the unknown elastic modulus and assuming Poisson's ratio (ν) to be ≈ 0.5.

* In the above context, a glass transition refers to the transition of a primarily viscous material into a primarily elastic amorphous solid via molecular coalescence with drying.

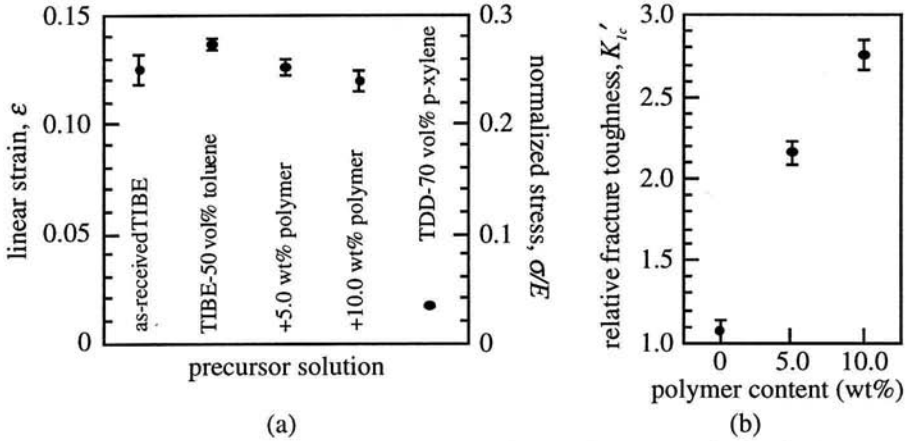

Fig. 4. (a) Linear strain and normalized internal stress calculated for each precursor film. (b) Relative (to that of TIBE alone) fracture toughness estimated for TIBE films with added polymer. Error bars correspond to the approximate range of error in determining the time to glass transition and measuring the critical thickness.

The internal strain and stress were nearly identical for all TIBE films, but were nearly ten times lower for the TDD film (Fig. 4a). Recall that the TIBE films cracked readily, and the TDD film did not crack at all. Also, recall that TIBE films lost significant mass during drying and the TDD film lost negligible mass. Since the TDD film showed relatively little evaporation, relatively little stress developed in the film. Thus, film cracking was prevented (increased critical film thickness) by choosing a precursor that minimized evaporative stresses during drying.

The film fracture toughness was calculated with Eq. (3) using: $\Omega = 1$ for the case $E << E_s$,[11] the measured critical film thickness, and the estimated internal film stress normalized to the unknown elastic modulus. To allow comparison between films, a relative fracture toughness (K_{Ic}') was calculated by dividing the elasticity normalized fracture toughness by that of the as-received TIBE film, which exhibited the least resistance to cracking. The relative film fracture toughness calculated for precursor films is shown in Table I. Solvent choice and dilution showed little effect on the film fracture toughness. The relative fracture toughness for the TDD film could not be determined since there was no observed cracking.

The relative film fracture toughness increased with increasing polymer content (Table I). Fig. 4b shows a greater than two-fold increase in relative fracture toughness for TIBE films with small additions of polymer. Recall that the extent of cracking decreased and the critical thickness increased with increased polymer content in TIBE films. The polymeric molecules are speculated to have toughened films of smaller, monomeric metal-organic molecules by providing a more cohesive network via molecular entanglements. Moreover, film cracking was prevented (increased critical film thickness) by adding elastomeric polymers to the precursor to increase the film fracture toughness.

Table I. Experimental and Calculated Results for Precursor Films

Precursor Solution*	h_c (μm)	t_g (min)	ε	σ/E	K_{Ic}'
TIBE-50% toluene	≈0.11	25-30	≈0.14	≈0.27	≈1.1
TIBE-50% toluene+5% polymer#	≈0.51	25-35	≈0.13	≈0.25	≈2.2
TIBE-50% toluene+10% polymer#	≈0.92	25-35	≈0.12	≈0.24	≈2.8
TDD-70% xylene	>50	20-30	≈0.02	≈0.03	–
TIBE-50% xylene	≈0.17	25-30	≈0.12	≈0.25	≈1.2
as-received TIBE	≈0.10	30-40	≈0.13	≈0.25	1.0

* solvent in vol% relative to precursor and polymer in wt% relative to precursor

Kraton® D1102C, a styrene-butadiene-styrene block copolymer

Closing Remarks

The above experimental and analytical methods comprise a simple approach to study cracking in thin films. Admittedly, several shortcomings persist in the simplified analysis presented in this paper and are discussed below. However, the ability of the approach to compare behavior and elucidate the important effects on film cracking was demonstrated. The demonstrated means of preventing film cracking were consistent with those described in the literature.[1,6] Thus, the approach in this study is viewed by the authors as a foundation to build more refined and accurate analyses upon.

The analysis in this study included the following assumptions: biaxial stress, linear elastic fracture mechanics, isotropic and constant elastic properties, no substrate deformation, perfect adhesion, minimal viscoelastic stress relaxation, and constant stress through the film thickness. The random crack patterns observed in all films validated the assumption of biaxial stress. The use of linear elastic fracture mechanics is justified as long as the plastic (or non-elastic) zone is small relative to the crack velocity. However, other assumptions should be improved upon.

In the present analysis, the only governing factor for the magnitude of internal film stress was the volume change due to evaporation after the film began to behave primarily elastically. Viscoelastic stress relaxation (especially at a crack tip) was ignored in the calculations. However, the scratch test appeared to capture at least some of the effects of stress relaxation, shown by a decreasing internal film stress with increasing polymer content (Fig. 4b). Ideally, either the viscoelastic film properties or film stress should be measured. Several techniques have been used to measure film stress from substrate deflections.[18-21] With the addition of stress measurement, a better assessment of thin film fracture toughness could be made.

If the calculations in this study were carried out to exact numerical solutions assuming an elastic modulus of 1 GPa, the internal stress and fracture toughness in films of this study were on the order of tens to hundreds MPa, and tens to hundreds $kPa \cdot m^{1/2}$, respectively. These values are believed to be an upper bound, because stress relaxation effects were not explicitly considered. Values reported in literature also suggest these stresses may be a slightly high estimate.[5,6,9] On the other hand, there are currently no known studies to compare thin film fracture toughness values. While exact calculations were not emphasized in this study, the use of simpler systems with well documented properties could facilitate such an objective.

ACKNOWLEDGMENTS

This work was supported by the National Science Foundation grant DMR-9623744. The authors thank Dr. Keith J. Bowman for helpful suggestions.

REFERENCES

1. C.J. Brinker, A.J. Hurd, P.R. Schunk, G.C. Frye and C.S. Ashley, "Review of Sol-Gel Thin Film Formation," *J. Non-Cryst. Solids*, **147-148**, 424-436 (1992).
2. G.W. Scherer, "Recent Progress in Drying of Gels," *J. Non-Cryst. Solids*, **147-148**, 363-374 (1992).
3. A. Atkinson and R.M. Guppy, "Mechanical Stability of Sol-Gel Films," *J. Mat. Sci.*, **26**, 3869-3873 (1991).
4. S.-Y. Chen and I-W. Chen, "Cracking during Pyrolysis of Oxide Thin Films–Phenomenology, Mechanisms, and Mechanics," *J. Am. Ceram. Soc.*, **78** [11] 2929-2939 (1995).
5. S. Bec, A. Tonck and J-L. Loubet, "Mechanical Properties of Pyrolytic "SiOCN" Thin Coatings," *Mat. Res. Soc. Symp. Proc.*, **308**, 577-582 (1993).
6. K. Sato, "The Internal Stress of Coating Films," *Progr. Org. Coatings*, **8**, 143-160 (1990).
7. M.D. Thouless, "Some Mechanics for the Adhesion of Thin Films," *Thin Solid Films*, **181**, 397-406 (1989).
8. G.P. Bierwagon, "Film Formation and Mudcracking in Latex Coatings," *J. Coatings Techn.*, **51** [658] 117-126 (1979).
9. S.G. Croll, "The Origin of Residual Internal Stress in Solvent-Cast Thermoplastic Coatings," *J. Appl. Polym. Sci.*, **23**, 847-858 (1979).
10. A.G. Evans, M.D. Drory and M.S. Hu, "The Cracking and Decohesion of Thin Films," *J. Mater. Res.*, **3** [5] 1043-1048 (1988).
11. M.S. Hu and A.G. Evans, "The Cracking and Decohesion of Thin Films on Ductile Substrates," *Acta Met.*, **37** [3] 917-925 (1989).
12. R.K. Roeder and E.B. Slamovich, "The Critical Thickness of Thin Metal-Organic Precursor Films: Effect of Polymer Additions," submitted to *J. Am. Ceram. Soc.*
13. E.B. Slamovich and I.A. Aksay, "Hydrothermal Processing of $BaTiO_3$/Polymer Films," *Mater. Res. Soc. Symp. Proc.*, **346**, 63-68 (1994).
14. E.B. Slamovich and I.A. Aksay, "Structure Evolution in Hydrothermally Processed (<100°C) $BaTiO_3$ Films," *J. Am. Ceram. Soc.*, **79** [1] 239-247 (1996).
15. A.S. Shaikh and G.M. Vest, "Kinetics of $BaTiO_3$ and $PbTiO_3$ Formation from Metallo-organic Precursors," *J. Am. Ceram. Soc.*, **69**, 682-688 (1986).
16. A.S. Shaikh, R.W. Vest and G.M Vest, "Dielectric Properties of Ultrafine Grained $BaTiO_3$," *IEEE Trans. UFFC*, **36** [4] 407-412 (1989).
17. Personal communication, Gelest Inc., Tullytown, PA.
18. J.H.L Voncken, C. Lijzenga, K.P. Kumar, K. Keizer, A.J. Burggraaf and B.C. Bonekamp, "New Method for the Measurement of Stress in Thin Drying Gel Layers Produced During the Formation of Ceramic Membranes," *J. Mater. Sci.*, **27**, 472-478 (1992).
19. K.E. Boggs, D.L. Wilcox, D.A. Payne and L.S. Allen, "Stress Development During High Dielectric Ceramic Thin Films Processing," *Proc. SPIE Int. Soc. Opt. Eng.*, **2256**, 350-355 (1994).
20. R.C. Chiu and M.J. Cima, "Drying Behavior of Granular Ceramic Films," *Ceram. Trans.*, **22**, 347-356 (1991).
21. T.J. Garino and M. Harrington, "Residual Stress in PZT Thin Films and Its Effect on Ferroelectric Properties," *Mater. Res. Soc. Symp. Proc.*, **243**, 341-347 (1992).